Available online at www.sciencedirect.com
SCIENCE DIRECT®
Computers and Chemical Engineering 27 (2003) 1855–1866
Computers & Chemical Engineering
www.elsevier.com/locate/compchemeng

Reactive distillation for methyl acetate production

Robert S. Huss, Fengrong Chen, Michael F. Malone, Michael F. Doherty *

Department of Chemical Engineering, University of Massachusetts, Amherst, MA 01003, USA

Received 6 December 2002; accepted 12 June 2003

Abstract

We describe a hierarchy of methods, models, and calculation techniques that support the design of reactive distillation columns. The models require increasingly sophisticated data needs as the hierarchy is implemented. The approach is illustrated for the production of methyl acetate because of its commercial importance, and because of the availability of adequate published data for comparison. In the limit of reaction and phase equilibrium, we show (1) the existence of both a minimum and a maximum reflux, (2) there is a narrow range of reflux ratios that will produce high conversions and high purity methyl acetate, and (3) the existence of multiple steady states throughout the entire range of feasible reflux ratios. For finite rates of reaction, we find (4) that the desired product compositions are feasible over a wide range of reaction rates, up to and including reaction equilibrium, and (5) that multiple steady states do not occur over the range of realistic reflux ratios, but they are found at high reflux ratios outside the range of normal operation. Our calculations are in good agreement with experimental results reported by Bessling et al., [Chemical Engineering Technology 21 (1998) 393].

Keywords: Reactive distillation; Design; Simulation; Methyl acetate

1. Introduction

The production of methyl acetate is a classic example of successful reactive distillation technology (Agreda & Partin, 1984; Agreda, Partin, & Heise, 1990). Soon after the invention and commercial application of this technology for methyl acetate synthesis it was used as a model system for testing a new design and synthesis framework that was developed for the limiting case of equilibrium chemical reactions, i.e. fast reactions or large holdups (Barbosa & Doherty, 1988a; Barbosa & Doherty, 1988b). In recent years, the focus of research has turned to kinetically controlled reactive distillations and the kinetics of methyl acetate synthesis have been studied extensively for both homogeneously and heterogeneously catalyzed reactions (Ronnback et al., 1997; Xu & Chuang, 1997; Song, Venimadhavan, Manning, Malone, & Doherty, 1998; Popken, Gotze, & Gmehling, 2000). Methods have also been developed recently for the design, synthesis, and feasibility analysis of kinetically controlled reactive distillation, and methyl acetate synthesis has commonly been used as a model system (Ismail, Proios, & Pistikopoulos, 2001; Lee & Westerberg, 2001; Chadda, Malone, & Doherty, 2001; Chadda, Doherty, & Malone, 2002). Extensive experimental data have been reported for many different configurations of reactive distillation devices for methyl acetate synthesis, which provides a good database for testing design and simulation models, e.g. Song et al., 1998; Bessling, Löning, Ohligschläger, Schembecker, & Sundmacher, 1998; Popken, Steinigeweg, & Gmehling, 2001. These studies also contain extensive literature reviews with special reference to methyl acetate synthesis. For an excellent general review of reactive distillation modeling, see Taylor & Krishna (2000).

In this article, we describe a hierarchy of methods, models, and calculation techniques that have been developed to support the design of reactive distillation columns. The models, which are hierarchical, require increasingly sophisticated data needs as the hierarchy is implemented. Methyl acetate synthesis is used as a model system to demonstrate the approach. The results

* Corresponding author. Present address: Department of Chemical Engineering, University of California, Santa Barbara, CA 93106-5080, USA. Tel.: +1-805-893-5309; fax: +1-805-893-4731.
E-mail address: mfd@engineering.ucsb.edu (M.F. Doherty).

0098-1354/03/$ - see front matter © 2003 Elsevier Ltd. All rights reserved.
doi:10.1016/S0098-1354(03)00156-X

Nomenclature

$a_{j,i}$	activity of component i on stage j
D	scaled Damköhler number ($=Da/(Da+1)$)
Da	Damköhler number for whole column
F_j	feed flow rate to stage j (zero for non-feed stages) (kmol/h)
H_j	holdup of stage j (kmol)
H_T	total holdup for the entire column (kmol)
H_T^R	total holdup with reaction(s) for the entire column (kmol)
K_{eq}	thermodynamic reaction equilibrium constant for a single reaction
K_r	thermodynamic reaction equilibrium constant of reaction r
$k_{f,r}$	forward rate constant of reaction r (h^{-1})
$k_{f,ref}$	forward rate constant evaluated at boiling point of a reference component (h^{-1})
L_j	liquid rate of stage j (kmol/h)
r	reflux ratio
s	reboil ratio
V_j	vapor rate of stage j (kmol/h)
x_i	liquid mole fraction of component i
$x_{j,i}$	liquid mole fraction of component i on stage j
X_i	transformed liquid mole fraction of component i
$y_{j,i}$	vapor mole fraction of component i on stage j
$z_{j,i}$	feed mole fraction of component i on stage j
Greek letters	
$\varepsilon_{j,r}$	extent of reaction r on stage j (mole reacted/(mole of mixture × time))
$\nu_{r,i}$	stoichiometric coefficient of component i in reaction r

show the effects of reflux ratio and kinetic parameters on the conversion in reactive distillation, in good agreement with measurements reported for this system by Bessling et al. (1998). This approach provides, we believe for the first time, a comprehensive understanding of the effect of kinetics in comparison to such experiments, as well as a demonstration of solution multiplicity in a reactive distillation system for esterification.

Methyl acetate (MeOAc) can be made by the liquid-phase reaction of acetic acid (HOAc) and methanol (MeOH) in the presence of an acid catalyst (e.g., sulfuric acid, or a sulfonic acid ion exchange resin) at a pressure of 1 atm. The reaction is

$$\mathrm{HOAc} + \mathrm{MeOH} \leftrightarrow \mathrm{MeOAc} + \mathrm{H_2O} \tag{1}$$

An activity-based rate model for the reaction chemistry is

$$r = k_f\left(a_{\mathrm{HOAc}}a_{\mathrm{MeOH}} - \frac{a_{\mathrm{MeOAc}}a_{\mathrm{H_2O}}}{K_{eq}}\right) \tag{2}$$

where the reaction equilibrium constant and the forward rate constant are given by:

$$K_{eq} = 2.32\,\exp\left(\frac{782.98}{T}\right) \tag{3}$$

$$k_f = 9.732\times 10^8\,\exp\left(-\frac{6287.7}{T}\right)\ \mathrm{h}^{-1} \tag{4}$$

where T is in K. The reaction equilibrium constant was taken from Song et al. (1998) and the rate constant in Eq. (4) was obtained by fitting the pseudo-homogeneous rate equation (2) to the heterogeneous rate data in Song et al. (1998). A typical fit is shown in Fig. 1. The heat of reaction used in this work is -3.0165 kJ/mol, indicating a slightly exothermic reaction, typical for acetate esterifications.

The liquid-phase activity coefficients are well represented by the Wilson equation. The required thermodynamic data for phase equilibrium in this system are given in Appendix A.

2. Equilibrium design

The first step in the procedure is to develop a spectrum of designs at phase and reaction equilibrium using the methods and reaction–invariant compositions developed by Barbosa and Doherty (1988a,b) and Ung and Doherty (1995a); Ung and Doherty (1995b,c,d). The reaction–invariant compositions exploit the reduction in degrees of freedom due to equilibrium reaction, allowing visualization of this system in two dimensions. The composition transformations for this system are:

$$X_A = x_{\mathrm{HOAc}} + x_{\mathrm{MeOAc}} \tag{5}$$

$$X_B = x_{\mathrm{MeOH}} + x_{\mathrm{MeOAc}} \tag{6}$$

where X_A represents the fractional molar composition of acetate groups (OAc), and X_B represents the fractional molar composition of alcohol groups (OH) in the

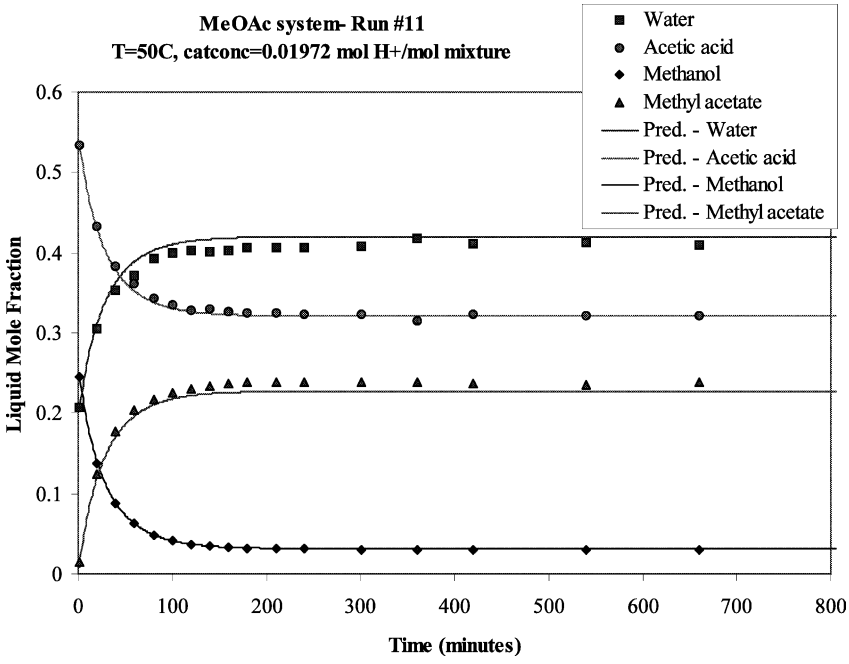

Fig. 1. Sample fit of pseudo-homogeneous rate model to experimental data, $k_f = 4.044$ (h^{-1}).

mixture. This phase of the design can be accomplished without the need for a reaction rate model, and can be carried out before the development of a rate model.

Fig. 2 shows three possible equilibrium reactive column designs, using the reaction–invariant compositions. The square is a projection of the reaction equilibrium surface onto two dimensions; each corner of the square represents a pure component, and each edge represents a non-reactive binary mixture. In these designs, all stages are at phase and reaction equilibrium.

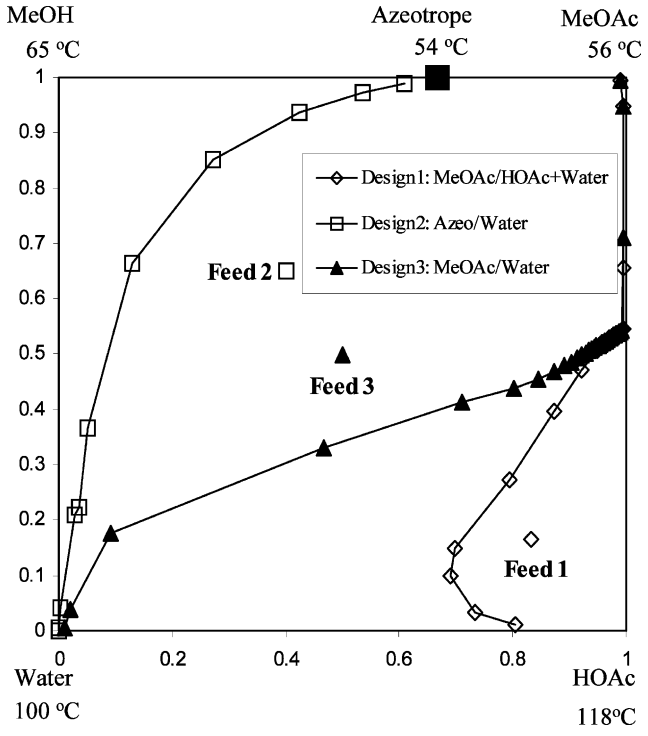

Fig. 2. Equilibrium designs. Feed 3 represents the overall composition of the two individual feed streams.

The first design, shown by the open diamonds, is a single-feed column similar to the example presented by Barbosa and Doherty (1988a,b). This column produces methyl acetate as a distillate, but uses an excess of acetic acid in the feed, and, therefore, has a bottoms stream consisting of water and acetic acid.

The second design, shown by the open squares, is also a single-feed column and could be a conceptual starting point for the Eastman column (Agreda & Partin, 1984). One interpretation of the Eastman column is that simultaneous reaction and separation occurs in the catalytic section (i.e., below the feed point for the sulfuric acid catalyst) producing water as a bottom product and the methanol/methyl acetate azeotrope in the vapor stream leaving the top of this section. This stream then enters a (non-reactive) extractive section placed on the top of the reactive column, which purifies the methyl acetate and forces the methanol down into the reaction zone.

The third design is a novel reaction equilibrium device with two feeds, where acetic acid is fed near the top of the column and methanol near the bottom in equimolar amounts (Huss, Song, Malone, & Doherty, 1997; Bessling et al., 1998). The column simultaneously produces methyl acetate as distillate, and water as bottom product. In this design, the rectifying section is a non-reactive extractive section separating methyl acetate and acetic acid. This can be seen from the rectifying profile in Fig. 2, which lies on the non-reactive edge between methyl acetate and acetic acid (note that

this is an output from the design model, not an input to it). It became apparent that this design was possible while we developed a two-feed version of design 2, and found that the middle-section trajectories reached this non-reactive edge.

Fig. 3 shows the effect of reflux ratio on the number of equilibrium reactive stages in this column design at a pressure of 1 atm. There is a minimum reflux at $r \sim 1.3$, and a maximum reflux at $r \sim 2.8$. Outside this range of reflux ratios, even an infinite number of equilibrium reactive stages will not accomplish the desired separation. Fig. 3b show some of the possible middle-section trajectories. Fig. 3b (top and bottom) show what occurs when the reflux ratio is too low and too high, respectively. There are an infinite number of stages at r_{min} because of a saddle pinch in the middle profile, and an infinite number of stages at r_{max} because of a node pinch in the middle profile. Fig. 3b (middle) shows the best middle profile to minimize the total number of stages in the column. A similar effect has been shown experimentally by Bessling et al. (1998).

Fig. 3a shows the effect of pressure on the range of feasible reflux ratios and stage requirements. Increasing the pressure increases the minimum number of stages required and reduces the range of feasible reflux ratios. Designs with a practical number of stages are not possible at pressures greater than ~ 1 atm, and are not even feasible at pressures greater than ~ 1.3 atm. We will consider the effect of pressure again when we include a side reaction in a later section.

In the final equilibrium design, we specified a methyl acetate mole fraction of 0.985 in the distillate, a water mole fraction of 0.985 in the bottoms, and a pressure of 1 atm. The reflux ratio that corresponds to the smallest number of reactive stages is $r = 1.7$, which is chosen as the base-case design value. The corresponding reboil ratio is $s = 2.7$ and there are $N = 38$ stages, each with an equilibrium chemical reaction (as noted earlier, the two stages in the rectifying section have essentially no reaction, so the effective number of chemical equilibrium stages is 36). A schematic of this column and the flow rates are shown in Fig. 4. The feed rates are based on the published production rate of 400 million lb per year of MeOAc (~ 280.0 kmol/h; Agreda et al., 1990).

3. Feasibility of kinetically controlled column

Before attempting to design a column away from the reaction equilibrium limit, we determine the feasibility of kinetic column operation using the procedure developed by Chadda et al. (2001, 2002). This method tracks fixed points of the rectifying and stripping sections starting from the non-reactive pure components and azeotropes, performing a bifurcation study with a Damköhler number (Da) as the continuation parameter.

The Damköhler number is the ratio of a characteristic process time (H_T^R/F) to a characteristic reaction time ($1/k_{f,ref}$). The normal boiling point of MeOAc is chosen as the reference temperature for the calculation of $k_{f,ref}$, giving a value of 5.1937 h^{-1} for a characteristic time of approximately 12 min. Da is 0 at the non-reactive limit and infinite at the reaction equilibrium limit. To avoid dealing with very large numbers, we present the results

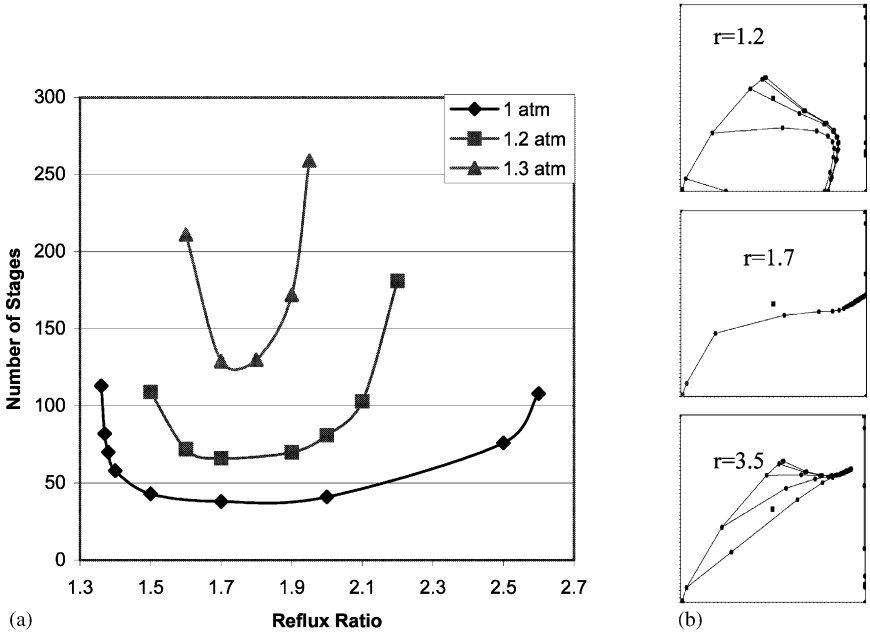

Fig. 3. Effect of reflux ratio on equilibrium design. Part (a) shows the number of stages required as a function of reflux ratio for three pressures. Part (b) shows the column trajectories for three different values of the reflux ratio at a pressure of 1 atm.

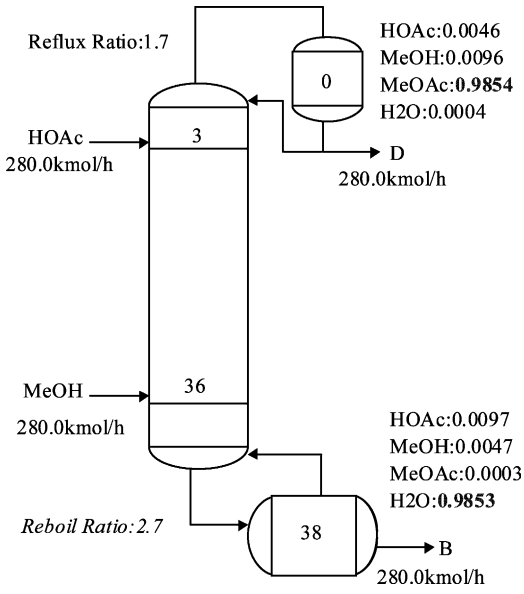

Fig. 4. Equilibrium design at 1 atm pressure. Compositions are reported in mole fractions.

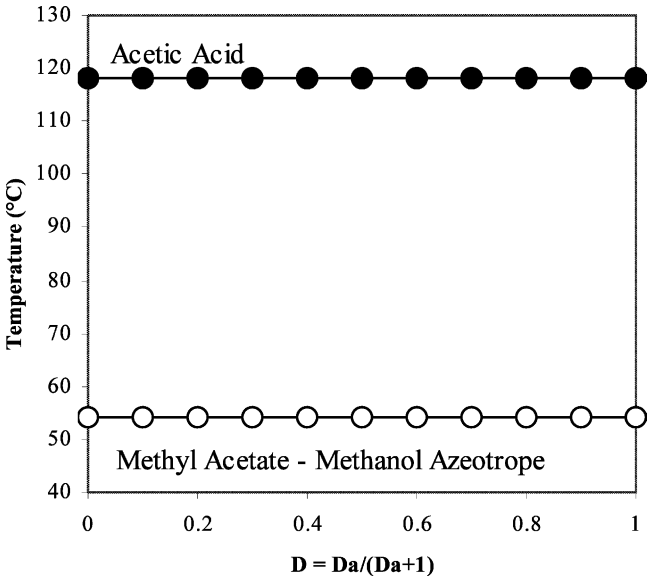

Fig. 5. Feasibility diagram. Filled circles are the potential bottom products (stable node branch in the stripping cascade) and open circles are the potential distillate products (unstable node branch in the rectifying cascade).

in terms of a scaled Damköhler number, D

$$D = \frac{Da}{1 + Da} \tag{7}$$

The fixed-point equations for the stripping cascade, and for the rectifying cascade are given by Eqs. (8) and (9), respectively.

$$0 = (1 - D)(x_i - y_i) + \frac{1}{k_{\mathrm{f,ref}}}\left(\frac{D}{\phi}\right)\sum_{r=1}^{R}(v_{r,i}\varepsilon_r) \tag{8}$$

$$0 = (1 - D)(x_i - y_i) - \frac{1}{k_{\mathrm{f,ref}}}\left(\frac{D}{\phi}\right)\sum_{r=1}^{R}(v_{r,i}\varepsilon_r) \tag{9}$$

We calculate the fixed points using an arc-length continuation procedure starting at the non-reactive azeotropes and pure components at $D = 0$, which are all known (Fidkowski, Malone, & Doherty, 1993). We track the branches and any bifurcated branches that may occur, to the reaction equilibrium limit at large values of D. This method also finds any reactive azeotropes that may exist at $D = 1$.

Fig. 5 shows the feasibility diagram for the methyl acetate system, i.e. the stable nodes in the stripping cascade, and the unstable nodes in the rectifying cascade. These branches represent feasible bottom products and distillate products, respectively. For the methyl acetate system, the fixed points correspond to acetic acid (bottoms) and the methyl acetate–methanol azeotrope (distillate). These feasible products remain the same throughout the entire kinetic regime up to the reaction equilibrium limit. Therefore, the desired separation (described in the previous section) that was found to be feasible at reaction equilibrium is also feasible at lower Damköhler numbers and the equilibrium design can be modified to achieve these products in a kinetically controlled column.

4. Kinetically controlled design/simulation

The next step in the procedure is to formulate a steady-state model for the kinetically controlled column, and to initialize it with the design developed at reaction equilibrium. The first-column simulation is performed at a large value of the Damköhler number in order to closely approximate reaction equilibrium conditions. Further simulations are performed at successively lower values of the Damköhler number until a realistic value is achieved. The column design is modified along the way in order to maintain the desired product purities.

The stage-to-stage steady-state material balances are formulated as a system of ordinary differential equations, which are integrated to steady state.

$$\frac{\mathrm{d}x_{j,i}}{\mathrm{d}\zeta} = (1 - D)\frac{H_{\mathrm{T}}}{H_j}\frac{1}{F} \times (F_j z_{j,i} + L_{j-1}x_{j-1,i} + V_{j+1}y_{j+1,i} - V_j y_{j,i} - L_j x_{j,i}) + D\frac{H_{\mathrm{T}}}{H_{\mathrm{T}}^{\mathrm{R}}}\frac{1}{k_{\mathrm{f,ref}}}\delta_j\sum_{r=1}^{R}(v_{r,i}\varepsilon_{j,r}) \tag{10}$$

We have found this formulation to be a stable and robust method for finding steady-state solutions. We refer to two formulations of this model, one with no heat effects and one with heat effects. The "heat-effects" model considers heat of reaction and non-constant heats

of vaporization in an adiabatic column. Chen, Huss, Malone, and Doherty (2000) described this model in detail.

A comparison of the reaction equilibrium design and a kinetic simulation at $Da = 100$ with the non-heat effects model (Chen et al., 2000) is shown in Fig. 6. This shows that the kinetic model approaches the reaction equilibrium design for high Damköhler number (they are closer at $Da = 1000$).

For the column operating near reaction equilibrium ($Da = 100$) simulations with increasing or decreasing reboil ratio, at a constant reflux ratio of 1.7, follow different branches of steady states as shown in Fig. 7. The resulting column composition and temperature profiles for the case where the reboil ratio is 2.7 are shown in Fig. 8, where the multiplicity is more easily seen. The initial estimates for composition and temperature profiles dictate whether a steady state simulation will converge to one solution or the other. Even though the temperature and composition profiles have a significant difference in the middle of the column, the conversion of both solutions is nearly identical.

Fig. 7 also shows a maximum in conversion at the base-case design ($s = 2.7$). This effect was first reported by Bessling et al. (1998), who also confirmed the result experimentally. The implications for column operation are quite significant: if a disturbance enters the process and causes the product purity to go off spec, then increasing the reboil ratio (or reflux ratio) will make the purity go even further off spec! Decreasing r or s also causes the purity to go further off spec. Therefore, column control must be achieved by strategies that are subtler than simply manipulating r or s individually.

This behavior is related to the existence of a maximum and minimum reflux ratio and the effect of reflux ratio on the total number of reactive stages, found with the column design method (Fig. 3). For a column with a

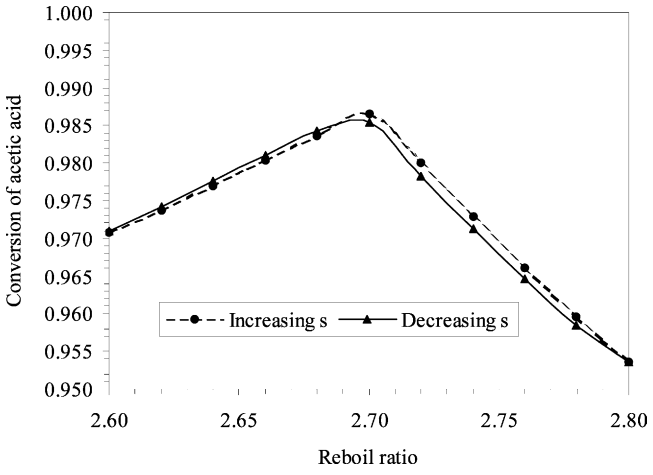

Fig. 7. Conversion of acetic acid as a function of reboil ratio for the reaction equilibrium design ($Da = 100$). The reboil ratio for the base-case design is $s = 2.70$.

fixed number of stages, this causes the product purities to fall-off as the reflux ratio (or reboil ratio) is either increased or decreased from its base-case design value.

Similar results have been found in other distillations that show both a minimum and maximum reflux, e.g., extractive distillation, Knapp and Doherty (1994) or reactive distillation, Okasinski and Doherty (1998).

Initially, to gain insight into an appropriate value of Da for realistic column operation, the transitions between the two limiting cases ($Da = 0$ and $Da = \infty$) are calculated using the non-heat effects model. We use this model initially because it is a simpler model that does not require as much physical property data to drive it. The conversion of acetic acid in the column, and average volume holdup per stage versus the Damköhler number are shown in Fig. 9. The average molar holdup on each stage is converted to a volume holdup using the average molar volume for the stage compositions. Fig. 9

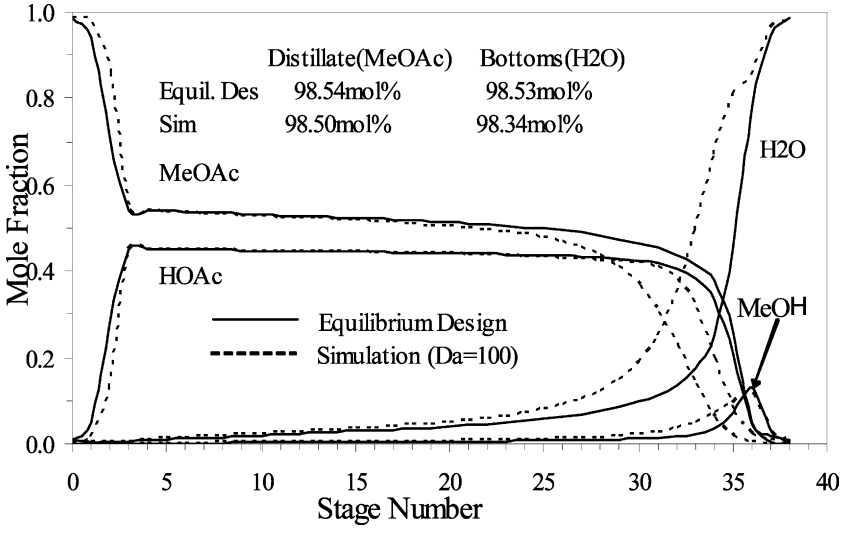

Fig. 6. Methyl acetate column. Comparison of column profiles between the simulation ($Da = 100$) and equilibrium design.

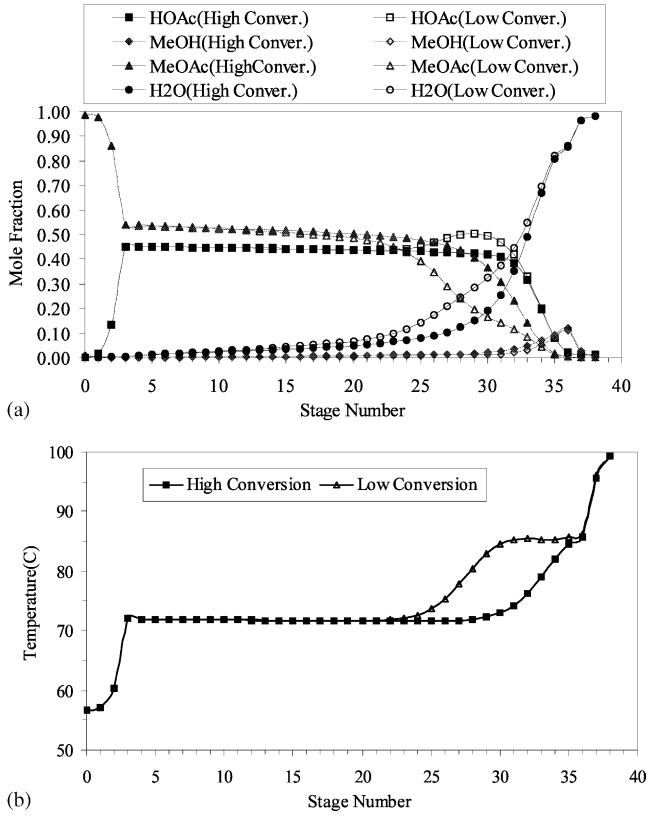

Fig. 8. Multiple steady states: column profiles at $r = 1.7$, $s = 2.7$, $Da = 100$. (a) Composition profiles; (b) Temperature profiles.

shows that the column simulation at $Da = 20$ is close to a realistic column operation because the purities of both products (distillate MeOAc: 98.24 mol% and bottoms H_2O: 97.25 mol%) are close to the design specifications, and the average volume holdup on each stage (~ 3 m^3) for the production rate of 400 million lb per year of MeOAc is reasonable. Therefore, we started with a value of $Da = 20$ to do further design and simulation.

At this point, we briefly summarize several design modifications described in detail in Huss, Chen, Malone, and Doherty (1999). In these steps, we made the top section of the column non-reactive, mainly because in the design at reaction equilibrium we find that this section performs essentially no reaction. This is consistent with the conceptual diagram of the Eastman column (Agreda et al., 1990). Since constant volume holdups are more practical to implement in a commercial column, we repeated the simulation with constant volume (3 m^3) rather than constant molar holdups.

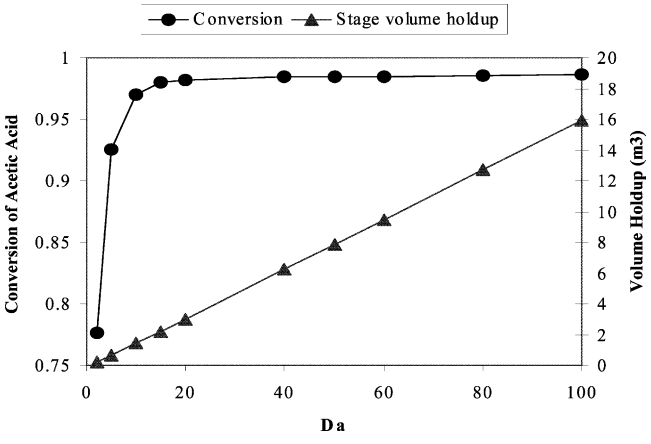

Fig. 9. Conversion of acetic acid and average stage volume holdup for different Da.

For the design policy in Fig. 10, the simulation results with the non-heat effects model show that this column produces product purities of 98.42 mol% MeOAc in the distillate and 97.11 mol% H_2O in the bottoms. These do not meet the design specifications. The calculated value of Da for this design is 17.5. By adding five reactive stages (three above and two below the MeOH feed stage) and increasing the reboil ratio from 2.7 to 2.73 (Huss et al., 1999), the simulation with the non-heat effects model shows that both products meet or exceed the design specification, shown in Fig. 11. We expect this to be close to a realistic design, which justifies the gathering of additional physical property data needed to drive the more sophisticated heat effects model which accounts for unequal latent heats, and heat of reaction.

The heat effects model is used for final simulations, starting with a simulation of the column shown in Fig. 11. We keep the distillate rate (281.547 kmol/h) and reflux ratio (1.7) constant. The predicted product purities, 98.35 mol% MeOAc in the distillate and 98.56 mol% H_2O in the bottoms, decreased only very slightly. Therefore, heat effects have no significant impact on the product purities for this system.

To determine whether the maximum in the conversion observed for reaction equilibrium operations persists away from reaction equilibrium, we also studied the influence of reflux ratio on the conversion of HOAc for the column in Fig. 11 with the heat effects model. The results are reported in Fig. 12. For these calculations, we held the distillate rate constant at a value of 281.547 kmol/h (this implies D/B is constant). The purities in both products exceed the design specification at $r = 1.9$ for reactive stage holdups of 3 m^3. Fig. 12 also shows that a maximum in conversion persists over a wide range of Damköhler numbers. As might be expected, higher conversions are obtained for higher Damköhler numbers (larger holdup of reacting liquid). However, for $Da > 20$, the gain in maximum conversion is very small compared to the required increase in Damköhler number. Therefore, adjusting Da is not a good strategy for improving the performance of the column. Once a column is built and the reacting liquid holdup and catalyst concentration are fixed (e.g. for a heterogeneous catalyst), the only way to change the Damköhler number is to change the feed flowrate to the column. To increase the maximum conversion from 0.986 to 0.989 requires the Damköhler number to be more than

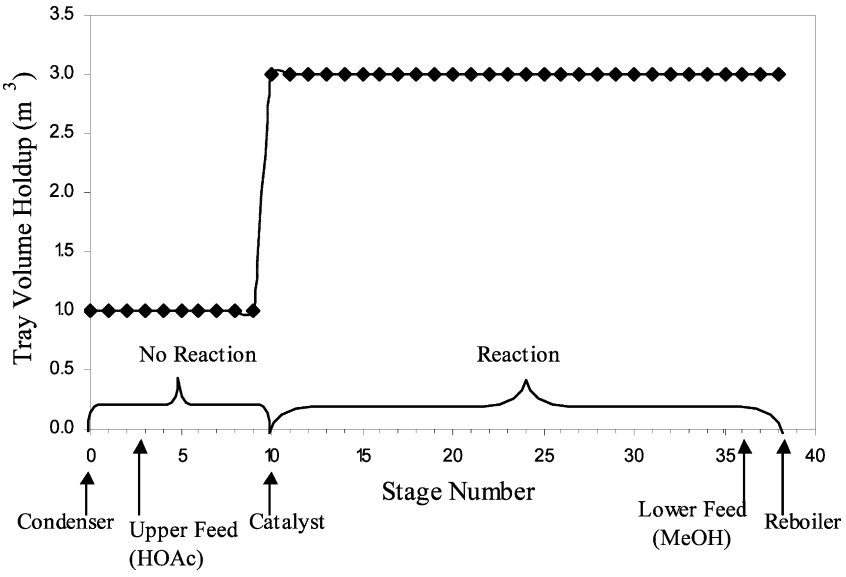

Fig. 10. Volume holdup distribution and reactive status throughout the column based on 400 million lb MeOAc per year (280.0 kg mol MeOAc/h).

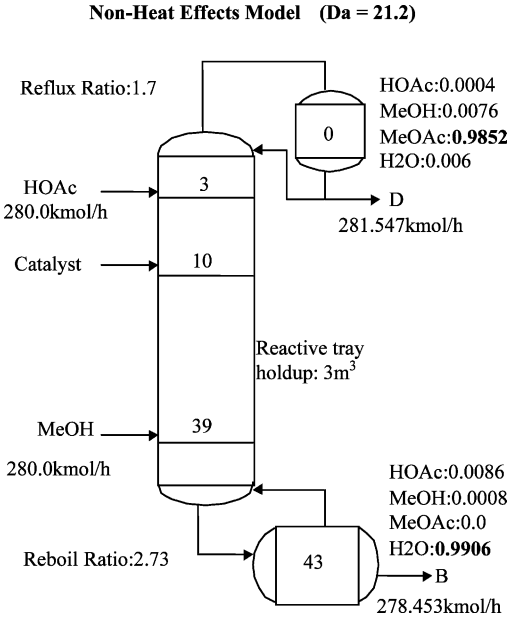

Fig. 11. Simulation summary using the non-heat effects model ($Da = 21.2$). Compositions are reported as mole fractions.

double, and to double the Damköhler number, the feed flowrate would need to be cut in half. This is clearly an undesirable control strategy. Adjusting the rate of addition for a homogeneous catalyst may be more effective.

Fig. 13 shows the final design/simulation summary, at $r = 1.9$. The profiles for the column in Fig. 11 and the column in Fig. 13 are quite similar, as shown in Fig. 14.

The forward/backward branches of steady states in the kinetic regime, calculated by increasing and decreasing the reflux ratio with constant volume holdup of 3 m^3 on each reactive stage ($Da \sim 21$) are reported in Fig. 15. It shows that the steady-state multiplicities occur for $r > 8$, which is outside the normally anticipated regime of column operation. This is in contrast to the equilibrium reactive design where multiplicities occur throughout the entire regime of column operation (Fig. 7). Therefore, finite rates of reaction have the important effect of eliminating multiple steady states from the regime of realistic operation for this chemistry.

5. Effects of side reaction

To study the effect of a side reaction on the selectivity and product purity, we account for the potential side reaction of methanol dehydrating to form dimethyl ether (DME) and water.

$$2\mathrm{MeOH} \Leftrightarrow \mathrm{DME} + \mathrm{H_2O} \tag{11}$$

and a rate expression is

$$r = k_f \left(a_{\mathrm{MeOH}}^2 - \frac{a_{\mathrm{DME}} a_{\mathrm{H_2O}}}{K_{eq}} \right) \tag{12}$$

The equilibrium constant and rate constant for Eq. (12) have been obtained from previous studies reported by (Song et al., 1998)

$$K_{eq} = 2.145 \exp\left(\frac{1239.8}{T}\right) \tag{13}$$

$$k_f = 7.602 \times 10^9 \exp\left(-\frac{10654}{T}\right) \mathrm{h}^{-1} \tag{14}$$

where T is in K. The normal boiling point of MeOAc is chosen as the reference temperature for the calculation of $k_{f,ref}$ (5.1937 h^{-1}) using the rate constant of the main reaction.

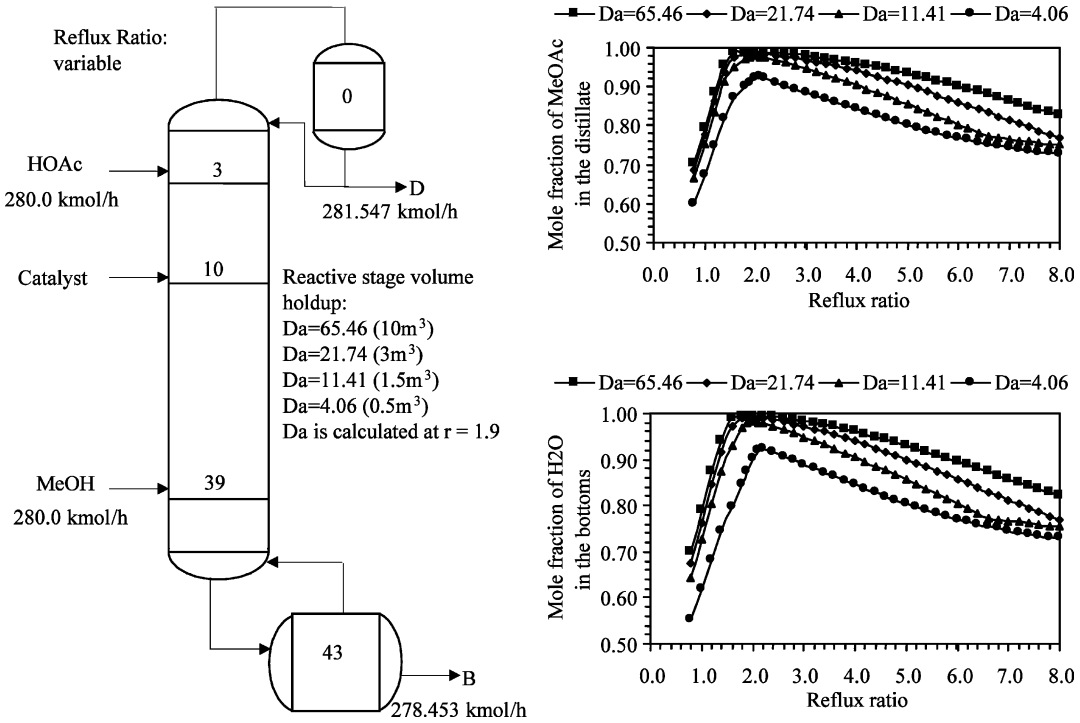

Fig. 12. Influence of reflux ratio on the compositions of MeOAc and H_2O in the distillate and bottoms, respectively, for different values of *Da*. Simulation with the heat effects model.

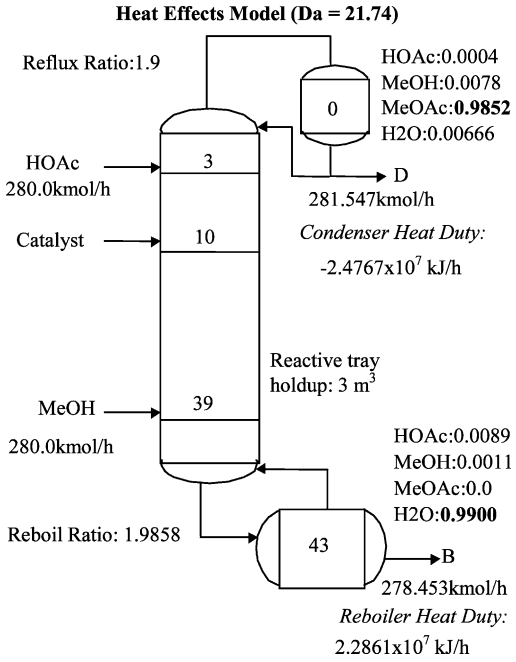

Fig. 13. Final design/simulation summary. Compositions are reported as mole fractions.

For the same specifications and column configuration described in Fig. 13, a simulation with the heat effects model and including the side reaction gives the results shown in Fig. 16. The results show no significant DME creation in the column at 1 atm. The side reaction may be more significant at higher pressures (because of higher boiling temperatures) but we found in our earlier calculations that higher pressure requires significantly more stages to achieve the same product compositions. Therefore, further study of this side reaction is not justified.

6. Comparison with experimental results

The detailed column configuration for this new simulation is taken from the test column of Bessling et al. (1998) (see Fig. 9 of Bessling et al., 1998). The comparison of our simulation results using our physical property and rate models with those experimental data is shown in Fig. 17 (note that similar results have been reported by Popken et al., 2001, see Fig. 8 in that article). For these calculations, we keep the distillate rate constant at 0.005 kmol/h (our estimate of the experimental value). The results show that the conversion of acetic acid in the column reaches a maximum of 96.48% at the optimal reflux ratio of 1.9 for the chemical equilibrium simulation ($Da = 100$). When the reflux ratio is higher than 1.9, the experimental data of Bessling et al. (1998) matches the simulation results for $Da = 27.5$. For values of $k_{f,ref} = 5.1937\ h^{-1}$ and $F = 0.01$ kmol/h (molar feed ratio methanol/acetic acid = 1:1), this value of $Da = 27.5$ implies an experimental column holdup of reacting liquid equal to 4 mol, or 2.0×10^{-4} m^3. This result agrees with the conclusion of Bessling et al. (1998, p. 399) that 'effects of chemical reaction

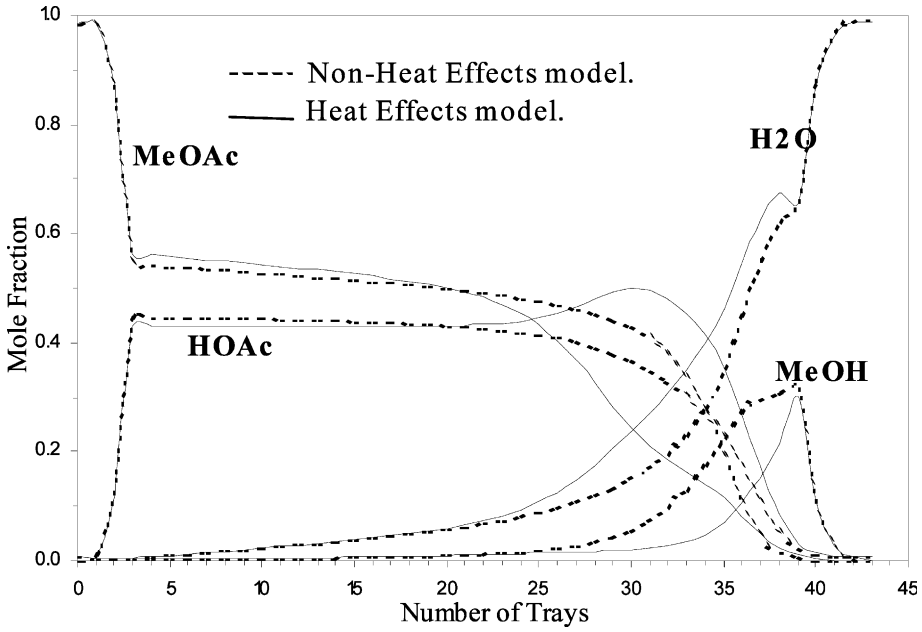

Fig. 14. Comparison of column profiles. Dotted line: profile of column in Fig. 11; stages 44; simulation with the non-heat effects model. Solid line: profile of column in Fig. 13; stages 44; simulation with the heat effects model.

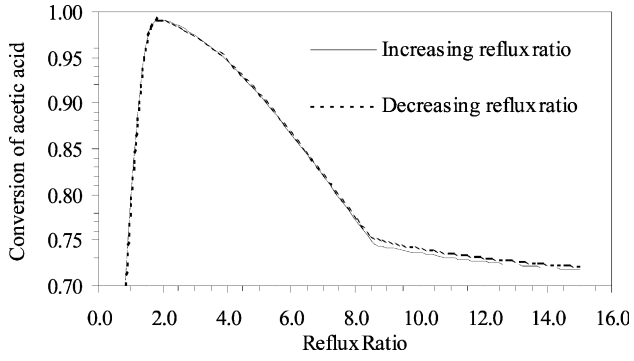

Fig. 15. Influence of reflux ratio on the conversion of acetic acid. 44 stages: feeds at stages 3, 39; stages 0–9, non-reactive; stages 10–43, reactive and constant volume holdup of 3 m^3 ($Da \sim 21$ for all the simulations); distillate rate was kept at 281.547 kmol/h for feed rates of 280.0 kmol HOAc/h and 280.0 kmol MeOH/h. Simulation with the heat effects model.

kinetics only become significant at higher reflux ratios in combination with a decreasing residence time of the reactants'.

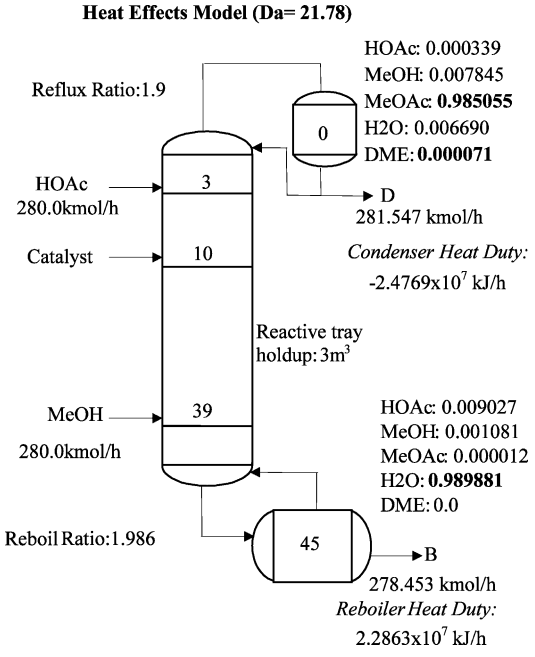

Fig. 16. Simulation summary with side reaction (DME). Compositions are reported as mole fractions.

7. Conclusions

We have explored a hierarchy of methods and models for the design and simulation of a reactive distillation column for the production of methyl acetate. We found that when assuming reaction equilibrium, it is possible to design a column operating with stoichiometric feeds and producing high-purity methyl acetate as distillate, and water as bottom product. For the reactive equilibrium column, we find an optimum value for the reflux ratio, producing a design with the minimum number of stages. With a higher or lower reflux ratio, the number of stages required increases. The feasible range of reflux ratios is small, and the feasible range decreases with increasing pressure.

We verified the equilibrium design with a kinetic simulation operating near the equilibrium limit. Sensitivity studies on this kinetic model reveal a region of multiple steady states around the optimum value of the

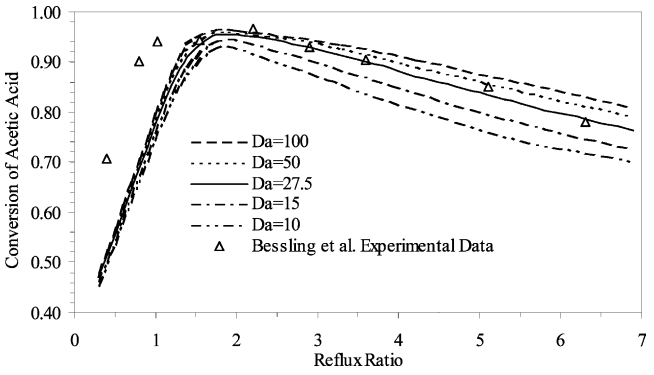

Fig. 17. Influence of reflux ratio on the conversion of acetic acid for different Da. The input data for the simulation are total number of stages = 27 including condenser (0) and reboiler (26); feed stage acetic acid = stage 7; feed stage methanol = stage 20; reactive section from stage 19 to stage 7; molar feed ratio methanol/acetic acid = 1:1; molar flow ratio $D/B = 1.0$; operating pressure, $P = 1$ atm. Simulation with the heat effects model.

reflux ratio. The two steady states produce nearly the same conversion, but have quite different temperature and composition profiles.

With a kinetic model, we performed a feasibility analysis and determined that the desired products are feasible over a wide range of Damköhler numbers, i.e., over a wide range of reaction rates, liquid holdups, production rates and catalyst concentrations. We used this information to develop a column design with realistic values for these design variables.

Sensitivity calculations for various Damköhler numbers showed that the conversion drops off sharply when operation moves away from the optimum reflux ratio. Furthermore, we found that increasing the Damköhler number yields an insignificant increase in conversion or operating range.

Finally, we compared our simulations to published experimental results for a reactive distillation column producing methyl acetate. Our findings match those in Bessling et al., 1998 quite closely.

Although this system is a commonly used example for reactive distillation research, and is one of the best examples of the benefits of using reactive distillation technology, we should note that it has some unique characteristics. It is the only system of the family of acetate esterification reactions that has no higher order azeotropes or liquid–liquid regions. The relative boiling points of the components make the acetic acid a candidate for use as an extractive agent. The extractive-reactive nature of this column produces a narrow operating range.

Acknowledgements

The authors are grateful for financial and technical support from the sponsors of the Fortune Project at the University of Massachusetts: Dow Corning Corp., DuPont Company, Eastman Chemical Company, ICI, Shell International Chemical BV, Union Carbide Corp., Hyprotech Ltd.

Appendix A: Thermodynamic data for methyl acetate system

A.1. Antoine coefficients

Component	A	B	C	V_i (cm^3/mol)
Acetic acid (1)	22.1001	−3654.62	−45.392	57.54
Methanol (2)	23.4999	−3643.3136	−33.434	44.44
Methyl acetate (3)	21.1520	−2662.78	−53.460	79.84
Water (4)	23.2256	−3835.18	−45.343	18.07
DME (5)	21.2303	−2164.85	−25.344	69.07

A.2. Wilson parameters

$A_{11} = 0.0$	$A_{12} = 2535.2019$	$A_{13} = 1123.1444$	$A_{14} = 237.5248$	$A_{15} = -96.7798$
$A_{21} = -547.5248$	$A_{22} = 0.0$	$A_{23} = 813.1843$	$A_{24} = 107.3832$	$A_{25} = 900.9358$
$A_{31} = -696.5031$	$A_{32} = -31.1932$	$A_{33} = 0.0$	$A_{34} = 645.7225$	$A_{35} = -17.2412$
$A_{41} = 658.0266$	$A_{42} = 469.5509$	$A_{43} = 1918.232$	$A_{44} = 0.0$	$A_{45} = 703.3566$
$A_{51} = 96.7797$	$A_{52} = -418.6490$	$A_{53} = -21.2317$	$A_{54} = 522.2653$	$A_{55} = 0.0$

$$\ln P^{\text{sat}} = A + \frac{B}{T + C}$$

where P^{sat} in Pa and T in K.

$$\ln \gamma_i = 1 - \ln\left(\sum_{j=1}^{C} x_j \Lambda_{ij}\right) - \sum_{k=1}^{C}\left(\frac{x_k \Lambda_{ki}}{\sum_{j=1}^{C} x_j \Lambda_{kj}}\right)$$

where

$$\Lambda_{ij} = \frac{V_j}{V_i}\exp\left(\frac{-A_{ij}}{RT}\right)$$

where V_j in cm^3/mol and A_{ij} in cal/mol.

$A_{ij} = 0$ implies ideality.

Dimerization constant in the vapor phase for acetic acid is

$$\log_{10}(K_{\text{D}}) = -12.5454 + \frac{3166.0}{T}$$

where K_{D} in Pa^{-1} and T in K.

References

Agreda, V.H., Partin, L.R. (1984). Reactive distillation process for the production of methyl acetate. U.S. Patent 4435595.

Agreda, V. H., Partin, L. R., & Heise, W. H. (1990). High-purity methyl acetate via reactive distillation. *Chemical Engineering Progess 86* (2), 40.

Barbosa, D., & Doherty, M. F. (1988a). Design and minimum reflux calculations for single-feed multicomponent reactive distillation columns. *Chemical Engineering Science 43*, 1523.

Barbosa, D., & Doherty, M. F. (1988b). Design and minimum reflux calculations for double-feed multicomponent reactive distillation columns. *Chemical Engineering Science 43*, 2377.

Bessling, B., Löning, J., Ohligschläger, A., Schembecker, G., & Sundmacher, K. (1998). Investigation on the synthesis of methyl acetate in a heterogeneous reactive distillation process. *Chemical Engineering Technology 21* (5), 393.

Chadda, N., Malone, M. F., & Doherty, M. F. (2001). Effect of chemical kinetics on feasible splits for reactive distillation. *American Institute of Chemical Engineering Journal 47*, 590.

Chadda, N., Doherty, M. F., & Malone, M. F. (2002). Feasibility and synthesis of hybrid reactive distillation systems. *American Institute of Chemical Engineering Journal 48*, 2754.

Chen, F., Huss, R. S., Malone, M. F., & Doherty, M. F. (2000). Simulation of kinetic effects in reactive distillation. *Computers and Chemical Engineering 24*, 2457.

Fidkowski, Z. T., Malone, M. F., & Doherty, M. F. (1993). Computing azeotropes in multicomponent mixtures. *Computers and Chemical Engineering 17*, 1141.

Huss, R.S., Song, W., Malone, M.F., Doherty, M.F. (1997) Computations and experiments for the feasibility of reactive distillation. Paper 199a, American Institute of Chemical Engineering Annual Meeting, Los Angeles, CA.

Huss, R. S., Chen, F., Malone, M. F., Doherty, M.F. (1999). Computer-aided tools for the design of reactive distillation systems. Computers and Chemical Engineering, S955.

Ismail, S. R., Proios, P., & Pistikopoulos, E. N. (2001). Modular synthesis framework for combined separation/reaction systems. *American Institute of Chemical Engineering Journal 47*, 629.

Knapp, J. P., Doherty, M. F. (1994). Minimum entrainer flows for extractive distillation. A bifurcation theoretic approach. *American Institute of Chemical Engineering Journal* 40, 243.

Lee, J. W., & Westerberg, A. W. (2001). Graphical design applied to MTBE and methyl acetate reactive distillation processes. *American Institute of Chemical Engineering Journal 47*, 1333.

Okasinski, M. J., & Doherty, M. F. (1998). Design method for kinetically controlled staged reactive distillation columns. *Industrial Engineering and Chemical Research 37*, 2821.

Popken, T., Gotze, L., & Gmehling, J. (2000). Reaction kinetics and chemical equilibrium of homogeneously and heterogeneously catalyzed acetic acid esterification with methanol and methyl acetate hydrolysis. *Industrial Engineering and Chemical Research 39*, 2601.

Popken, T., Steinigeweg, S., & Gmehling, J. (2001). Synthesis and hydrolysis of methyl acetate by reactive distillation using structured catalytic packings: experiments and simulation. *Industrial Engineering and Chemical Research 40*, 156.

Ronnback, R., Salmi, T., Vuori, A., Haario, H., Lehtonen, J., Sundqvist, A., & Tirronen, E. (1997). Development of a kinetic model for the esterification of acetic acid with methanol in the presence of a homogeneous acid catalyst. *Chemical Engineering Science 52*, 3369.

Song, W., Venimadhavan, G., Manning, J. M., Malone, M. F., & Doherty, M. F. (1998). Measurement of residue curve maps and heterogeneous kinetics in methyl acetate synthesis. *Industrial Engineering and Chemical Research 37*, 1917.

Taylor, R., & Krishna, R. (2000). Modelling reactive distillation. *Chemical Engineering Science 55*, 5183.

Ung, S., & Doherty, M. F. (1995a). Synthesis of reactive distillation systems with multiple equilibrium chemical reactions. *Industrial Engineering and Chemical Research 34*, 2555.

Ung, S., & Doherty, M. F. (1995b). Vapor–liquid phase equilibrium in systems with multiple chemical reactions. *Chemical Engineering Science 50*, 23.

Ung, S., & Doherty, M. F. (1995c). Theory of phase equilibrium in multi-reaction systems. *Chemical Engineering Science 50*, 3201.

Ung, S., & Doherty, M. F. (1995d). Calculation of residue curve maps for mixtures with multiple equilibrium chemical reactions. *Industrial Engineering and Chemical Research 34*, 3195.

Xu, Z. P., & Chuang, K. T. (1997). Effect of internal diffusion on heterogeneous catalytic esterification of acetic acid. *Chemical Engineering Science 52*, 3011.